


## ORIGINAL ARTICLE

# Hyaluronic acid vinyl esters: A toolbox toward controlling mechanical properties of hydrogels for 3D microfabrication

Elise Zerobin<sup>1,4</sup> | Marica Markovic<sup>2,4</sup> | Zuzana Tomášiková<sup>1,4</sup> |  
Xiao-Hua Qin<sup>1,4</sup> | Davide Ret<sup>1,4</sup> | Patrick Steinbauer<sup>1,3,4</sup> | Jakob Kitzmüller<sup>1,4</sup> |  
Wolfgang Steiger<sup>2,4</sup> | Peter Gruber<sup>2,4</sup> | Aleksandr Ovsianikov<sup>2,4</sup> |  
Robert Liska<sup>1,4</sup> | Stefan Baudis<sup>1,3,4</sup> 

<sup>1</sup>Institute of Applied Synthetic Chemistry, TU Wien, Vienna, Austria

<sup>2</sup>Institute of Materials Science and Technology, TU Wien, Vienna, Austria

<sup>3</sup>Christian Doppler Laboratory for Advanced Polymers for Biomaterials and 3D Printing, TU Wien, Vienna, Austria

<sup>4</sup>Austrian Cluster for Tissue Regeneration, Austria

## Correspondence

Stefan Baudis, Institute of Applied Synthetic Chemistry, TU Wien, Getreidemarkt 9, 1060 Vienna, Austria.  
E-mail: stefan.baudis@tuwien.ac.at

## Funding information

Bundesministerium für Digitalisierung und Wirtschaftsstandort; Österreichische Nationalstiftung für Forschung, Technologie und Entwicklung; Österreichische Forschungsförderungsgesellschaft, Grant/Award Numbers: 1362110, 849787

## Abstract

In this study, a thorough exploration of constitutional parameters of thiol-ene photocrosslinkable hydrogels based on hyaluronic acid vinyl ester was conducted in order to decipher their impact on material properties. These constitutional parameters originated from the process of synthesis (macromer size and degree of substitution) and from the process of formulation (photoinitiator concentration, macromer content, and thiol-to-ene ratio). Various macromers were obtained with a broad variety of degrees of substitution. Photoreology measurements were performed in order to determine the influence of the structure parameters on photoreactivity and the physical properties of hydrogels. Final crosslink densities and photoreactivities dramatically increase with increasing number of functional groups, macromer concentrations as well as with photoinitiator concentration. Swellabilities of the hydrogels were determined as complementary reference values. Mass swelling ratios as well as mass loss increased with decreasing degree of substitution as a result of increased mesh size and hydrophilicity. Finally, hyaluronic acid vinyl ester formulations were used to encapsulate fluorescent-labeled immortalized human adipose-derived mesenchymal stem cells in 3D via UV and by high-resolution two-photon polymerization. Cell-survival was successfully studied via confocal laser scanning microscopy during the course of 2 weeks.

## KEYWORDS

hyaluronic acid, biofabrication, cell encapsulation, Photopolymerization, two-photon polymerization

## 1 | INTRODUCTION

The extracellular matrix (ECM) forms the mechanical framework for living tissue and controls many functions

including tissue morphogenesis,<sup>[1]</sup> regulation of cell differentiation and proliferation,<sup>[2,3]</sup> and processes for regeneration after injuries<sup>[4]</sup> and is therefore a central consideration in the field of tissue engineering and

This is an open access article under the terms of the Creative Commons Attribution-NonCommercial License, which permits use, distribution and reproduction in any medium, provided the original work is properly cited and is not used for commercial purposes.

© 2020 The Authors. *Journal of Polymer Science* published by Wiley Periodicals, Inc.

regenerative medicine.<sup>[5,6]</sup> The ECM consists of two main components<sup>[7]</sup>—collagen fibers, which aggregate to bundles and extend through the stromal tissue and therefore provide durability, and the proteoglycan filaments, which are composed of protein chains in the core with covalently linked glycosaminoglycans (e.g., hyaluronic acid). These filaments interconnect cells and bind cations due to their carboxylate functionality. Hyaluronic acid (HA) is one of the major components of the ECM, particularly of soft connective tissue.<sup>[8]</sup> For this reason, research also concentrates on the applicability of HA in biomedicine.<sup>[9–13]</sup> In this context, the modification of HA to integrate more functions, such as trigger-able hydrogel formation or tailored degradation behavior, is of high importance. A common approach is chemical modification to form precursors for covalently crosslinked hydrogels. Here, HA-ene modifications were widely examined.<sup>[14–19]</sup> However, the inherent cytotoxicity of maleimides, norbornenes and especially (meth)acrylates is problematic. For this reason, vinyl ester were introduced as low toxicity substitutes for photopolymer systems.<sup>[20]</sup> These alternative functionality to form crosslinked polymers has already proved its applicability for hard tissue replacement<sup>[21]</sup> and recently also demonstrated its good performance in *in vivo* experiments.<sup>[22]</sup> We previously presented hyaluronic acid vinyl ester (HA-VE) as a novel class of naturally-derived precursor for hydrogels to approach soft tissue replacements.<sup>[23]</sup> Especially in comparison with HA acrylates or methacrylates HA-VEs showed increased biocompatibility. Moreover, application of thiol-ene chemistry<sup>[24]</sup> led to a tremendous increase of photoreactivity of the system to values comparable with acrylates.<sup>[25]</sup> Thiol-ene based polymer architectures have been extensively employed in literature to generate material platforms to direct the cell behavior, including human mesenchymal stem cells,<sup>[26]</sup> pancreatic  $\beta$ -cells,<sup>[27]</sup> fibroblasts and endothelial cells.<sup>[28]</sup> It was shown that hydrogels based on HA-VE are fully biodegradable with non-toxic degradation products.<sup>[23]</sup> In previous work, 3D hydrogel constructs with a very high resolution could be fabricated using two-photon polymerization (2PP).<sup>[29–31]</sup> 2PP is a sophisticated additive manufacturing technology (AMT), which enables the 3D printing of very complex structures in high resolution.<sup>[32]</sup> Two-photon absorption and photoinitiator activation, respectively, is only attained at high photon densities within the focal point of the femtosecond laser. Consequently, polymerization and solidification of the formulation are only induced in the voxel of the focal plane, but not occur along the path of the laser beam through the hydrogel precursor solution. Multiphoton processing has been widely used in literature to fabricate biocompatible 3D constructs based on collagen,<sup>[33]</sup> extracellular matrix

proteins,<sup>[34]</sup> bovine serum albumin,<sup>[35]</sup> and fibroin.<sup>[36]</sup> The range of structure parameter for HA-VE based hydrogels remained limited prohibiting the elucidation of detailed structure-properties relationships. Therefore, we widened the scope of examination in the present study in order to develop a profound understanding of interrelation of structure parameter and the material properties. The combinatorial synthesis of HA-VE provided a sufficient parameter space for this task. This study on different HA-VE species should provide greater clarity in understanding the versatile options available in the field of available hydrogel materials. The strong demand for a toolbox-material is met by the variation of the macromer size and degree of substitution, providing a deeper understanding in photoreactivity as well as mechanical properties of the resulting hydrogels. Finally, it is crucial to investigate the biocompatibility of HA-VE materials.

## 2 | EXPERIMENTAL

### 2.1 | Materials

Commercially available reagents and solvents within this study were purchased from Sigma-Aldrich or TCI and used as received unless noted otherwise. Hyaluronic acid sodium salt from *Streptococcus equi* ( $1.5\text{--}1.8 \times 10^6$  Da) was purchased from Sigma-Aldrich. Sodium hyaluronate (50–90 kDa) was purchased from Contipro (Czech Republic). Immortalized human adipose-derived mesenchymal stem cells (ASC) were purchased from Evercyte, Vienna, Austria (ASC/TERT1) and transfected with green fluorescent protein (ASC-GFP) as described in literature.<sup>[37]</sup> Endothelial Cell Growth Medium-2 (EGM-2) was used for ASC-GFP cells purchased from Lonza, Basel, Switzerland and supplemented with 10% fetal bovine serum (FBS). Trypsin–EDTA solution was purchased from Gibco (Waltham, MA). Glass surfaces were treated with 3-(trimethoxysilyl)propyl methacrylate purchased from Sigma-Aldrich according to the protocol provided.<sup>[38]</sup>

### 2.2 | Synthesis

The synthesis of HA-VEs with different macromer sizes and degrees of substitution (DS) was performed in a similar procedure as described previously.<sup>[23]</sup> HA with different molecular weight (m.w.) were either purchased or prepared by acidic degradation of HA ( $M_n \approx 1.5$  MDa, Fluka) by hydrochloric acid (0.1 M) in a 0.5 wt.% aqueous solution for 12 hr and 24 hr at 60 °C. Subsequently, the solution was neutralized (to a pH of 7.0, monitored by

pH meter) with aqueous sodium hydroxide (3 M) and dialyzed (m.w. cut-off 3.5 kDa, Carl Roth) against deionized water for at least 60 hr (with at least seven changes of water). Low m.w. HA sodium salt (96% th. after 12 hr and 49% th. after 24 hr) was obtained as a white solid by means of lyophilization. The sodium salt was dissolved in deionized water under gentle agitation to avoid solution degradation processes<sup>[39]</sup> and the 3 wt.% aqueous solution was stirred with 15 wt.% highly acidic ion-exchange resin (IR120, Amberlite) for 4 hr at r.t. After filtration, the solution was neutralized to a pH of 7.0 with tetrabutylammonium hydroxide (40 wt.% aqueous solution) and lyophilized to obtain HA tetrabutylammonium salt (HA-TBA, 92% th. for 12 hr degraded HA and 98% th. for 24 hr degraded HA) as a slightly pink solid. Finally, HA-VEs were obtained by the conversion of HA-TBA with a 15-fold excess of divinyl adipate (TCI GmbH) in an anhydrous dimethyl sulfoxide (DMSO) solution (4 wt.%) in a transesterification reaction at 50 °C for different time periods (24 hr, 96 hr, and 8 days). For the work-up, HA-VEs were precipitated in cold isopropyl alcohol, dialyzed against saline solution (48 hr with at least seven changes of solution) and against deionized water (72 hr, with at least seven changes of water), and lyophilized to obtain the products as white solids in yields of at least 80% th. <sup>1</sup>H NMR (400 MHz, 512 scans, D<sub>2</sub>O), δ [ppm]: 8.07 (d, xH, CH=CH<sub>2</sub>), 7.45 (d, xH, CH=CH<sub>2</sub>), 7.20 (q, xH, CH=CH<sub>2</sub>), 4.55–4.46 (d, 2H, C<sup>1</sup>H and C<sup>1</sup>H), 3.34–3.84 (m, 11H, [ring]CH and ring-CH<sub>2</sub>), 2.51 (bs, 4xH, CH<sub>2</sub>C(O)O), 2.02 (s, 3H, CH<sub>3</sub>C(O)N), 1.68 (bs, 4xH, CH<sub>2</sub>-CH<sub>2</sub>); x represents the degree of substitution (DS). <sup>1</sup>H NMR (400 MHz, 512 scans, D<sub>2</sub>O ± NaOD), δ [ppm]: 4.52–4.44 (d, 2H, C<sup>1</sup>H and C<sup>1</sup>H), 3.36–3.92 (m, 11H, [ring]CH and ring-CH<sub>2</sub>), 2.18 (t, 4xH, CH<sub>2</sub>C(O)O), 1.99 (s, 3H, CH<sub>3</sub>C(O)N), 1.54 (t, 4xH, CH<sub>2</sub>-CH<sub>2</sub>); x represents the degree of substitution (DS). <sup>1</sup>H NMR spectra of HA50VE05 are depicted in Figure S1. In the following the nomenclature HA(m.w.)VE(DS) was chosen for HA-VEs originating from HA with a certain m.w. and DS, for example, HA22VE95 was derived from HA with a m.w. of 22 kDa having a DS of 95% as determined via NMR.

### 2.3 | Characterization of macromers

<sup>1</sup>H NMR spectra were recorded at 25 °C in D<sub>2</sub>O (grade of deuteration ≥99.5%, Sigma-Aldrich) at 400 MHz using a Bruker Avance 400 Fourier transform spectrometer. The signal of non-deuterated H<sub>2</sub>O at 4.79 ppm was used as reference. Gel permeation chromatography (GPC) analysis was performed using a Viscotek GPC system, including a Viscotek GPCmax VE2001 GPC solvent/sample module (100 μl loop), a solvent degasser, a Viscotek

VE3580 refractive index concentration detector, a Waters precolumn, a Waters ultrahydrogel linear 7.8 × 30 mm column, and a Waters ultrahydrogel 250 7.8 × 30 mm column with 10 μm particle size. The eluent was Phosphate-buffered saline (NaH<sub>2</sub>PO<sub>4</sub> 0.05 M, NaCl 0.1 M, NaN<sub>3</sub> 0.05%) at a temperature of 30 °C and a flow rate of 0.5 ml min<sup>-1</sup>. Polyethylene glycol standards (American Polymer Standards Corporation) were used for standard calibration to determine the number average of the molecular weight ( $\bar{M}_n$ ) and the polydispersity ( $\bar{D}_M$ ).

### 2.4 | Photorheology

Photoreological measurements were performed on an Anton Paar Modular Compact Rheometer MCR 302 WESP with a plate-to-plate measuring system with a 25 mm steel stamp, a glass plate, and a gap size of 50 μm in oscillation mode with 10 Hz and an amplitude of 10% strain at 25 °C.<sup>[40]</sup> Samples were irradiated with filtered light (320–500 nm, EXFO Omnicure S2000) bottom-up through the glass plate with a light intensity of 3.2 W cm<sup>-2</sup> at the tip of the light guide as measured with an EXFO Omnicure R2000 radiometer. This referred to a light intensity of 40 mW cm<sup>-2</sup> directly above the glass plate. Storage modulus  $G'$  and loss modulus  $G''$  were measured every second; light was automatically activated after 60 seconds and the measurement was continued until a constant  $G'$  was attained.

### 2.5 | UV cell encapsulation

UV cell encapsulation was performed by mixing HA-VE based hydrogel precursor formulation in a 1:1 ratio (v/v) with a cell suspension in medium (ASC-GFP) to reach final concentrations of 15 wt.% HA50VE05/80 mol% (thiol-to-ene) dithiothreitol (DTT) and 0.5 mM lithium phenyl-2,4,6-trimethylbenzoylphosphinate (LiTPO).<sup>[41]</sup> Hydrogels were polymerized using silicone gaskets applied on glass cover slips. Labeled cells (ASC-GFP) were used enabling straightforward cell imaging without staining. All formulations were prepared in a laminar flow hood under sterile conditions. Cells were cultured and maintained in EGM-2 supplemented with 10% fetal bovine serum. Cells were incubated in humidified atmosphere at 37 °C with 5% CO<sub>2</sub>. Cells were detached using 0.5% trypsin-EDTA solution. Afterwards, cell culture medium with serum was added to inactivate trypsin. Cells were collected in Falcon tubes and centrifuged at 300 rpm (3 min). Cells were counted, spun down once more and resuspended in the calculated amount of polymer solution in order to reach final concentrations of 10<sup>6</sup>

cells  $\text{ml}^{-1}$ . Hydrogels were polymerized using Grace Bio-Labs CultureWell™ reusable gaskets (CW-8R-1.0, 8–6 mm diameter  $\times$  1 mm depth) and Boekel Scientific UV-crosslinker (1 J, 368 nm, 4 min). Gels were transferred to a sterile  $\mu$ -dish (ibidi GmbH, Germany), immersed in cell medium and incubated in a humidified atmosphere with 5%  $\text{CO}_2$  at 37 °C. Cell-survival was monitored via confocal laser scanning microscopy (LSM) (Zeiss, Germany), changing cell medium every day. The proliferation rate (cell number) was determined by counting the living cells using ImageJ within the recorded section and normalizing values on day 4, 11 and 14 to the data of day 1 (100%).

## 2.6 | Cell encapsulation by two-photon polymerization

Cell encapsulation experiments were performed by mixing equal parts (1:1, v/v) of a cell suspension in medium (ASC-GFP,  $10^6$  cells  $\text{ml}^{-1}$ ) with HA-VE based hydrogel precursor formulation to reach final concentrations of 5 wt.% HA22VE95/80 mol% DTT. The photoinitiator 3,3'-(((1E,1'E)-(2-oxocyclopentane-1,3-diylidene) bis(methanylylidene)) bis(4,1-phenylene)) bis(methylazanediy))dipropanoate (P2CK)<sup>[42]</sup> was used in a concentration of 0.5 mM. The formulation was pipetted into a surface-treated ibidi  $\mu$ -dish (35 mm with glass bottom, ibidi GmbH, Martinsried, Germany). Glass surfaces were treated with 3-(trimethoxysilyl)propyl methacrylate in order to avoid hydrogel detachment during incubation.<sup>[43]</sup> Another formulation was prepared by mixing equal amount (1:1, v/v) of hydrogel precursor formulation with the same amount of Dulbecco's Phosphate Buffered Saline (PBS) solution without calcium and magnesium in order to perform a cell-free control experiment. Microfabrication was performed by means of a two-photon polymerization (2PP) system. The used 2PP

system is based on a Ti:sapphire laser system (wavelength 800 nm, pulse width 70 fs, objective Olympus 10x/(NA 0.3), scanning speed 100  $\text{mm s}^{-1}$ , hatch 0.3  $\mu\text{m}$ , layer spacing 0.5  $\mu\text{m}$ ) and was also employed in a previous study.<sup>[44]</sup> A detailed description of the setup and the process can be found in literature.<sup>[29]</sup> Hydrogel structures (TU Wien Logos,  $100 \times 100 \times 100 \mu\text{m}$ ) were printed by scanning the focused laser beam with a writing speed of 100  $\text{mm s}^{-1}$  (triplicates) with varied laser power (10–150 mW, 10 mW steps) through the hydrogel precursor formulation according to the layer information from the sliced CAD file. The samples were developed in medium or PBS solution, respectively and remaining precursor solution was washed away. GFP-labeled cells (ASCs) were visualized by a confocal LSM 700 (Zeiss, Germany) using ZEN11 software for cell imaging. Viable cells emitted green fluorescence at excitation/emission set to 488/530 nm. After imaging, hydrogels were immersed in cell medium and incubated in a humidified atmosphere with 5%  $\text{CO}_2$  at 37 °C. Cell quantification was performed by counting the cells within the 4 divided groups using ImageJ on day 7 and normalizing the data to day 3 (100%) after encapsulation.

## 3 | RESULTS AND DISCUSSION

### 3.1 | Synthesis of vinyl ester functionalized hyaluronic acid

Vinyl ester (VE) functionalized hyaluronic acid (HA) with different macromer sizes and degrees of substitution were synthesized in a multi-step procedure.<sup>[23]</sup> Commercial high m.w. HA ( $1.5\text{--}1.8 \times 10^6$  Da) was degraded in acidic solution at 60 °C for 12 hr and 24 hr, respectively, in order to obtain two different low m.w. HA batches as confirmed by GPC measurements (Table 1). HA with a m.w. of 50 kDa was purchased and

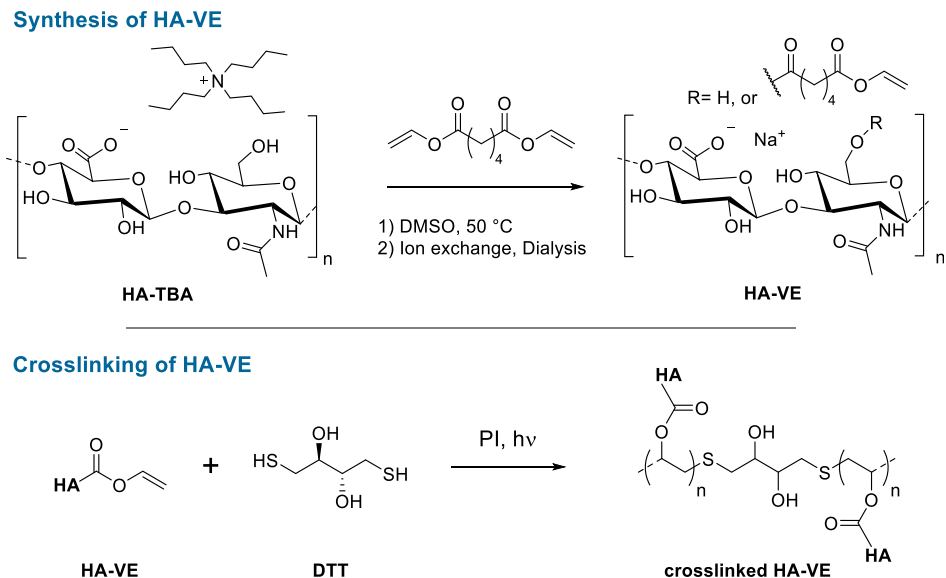
**TABLE 1** Overview on vinyl ester functionalized hyaluronic acids

| Macromer ID | HA-degradation time [h] | $\bar{M}_n/\bar{D}_M^a$ [kDa]/[] | DS <sup>b</sup> [%] | Yield [% th.] |
|-------------|-------------------------|----------------------------------|---------------------|---------------|
| HA22VE20    |                         |                                  | 20                  | 80            |
| HA22VE40    | 24                      | 22/2.4                           | 40                  | 93            |
| HA22VE95    |                         |                                  | 95                  | 99            |
| HA50VE05    | n.a.                    | 50/2.7                           | 5                   | 80            |
| HA80VE15    |                         |                                  | 15                  | 91            |
| HA80VE50    | 12                      | 80/1.9                           | 50                  | 81            |
| HA80VE80    |                         |                                  | 80                  | 91            |

<sup>a</sup>Number average molecular weight  $\bar{M}_n$  and polydispersity  $\bar{D}_M$  of degraded HA, determined by GPC.

<sup>b</sup>Average degree of substitution (DS) determined by <sup>1</sup>H NMR.

**FIGURE 1** Synthesis of hyaluronic acid vinyl esters (HA-VE, top) and schematic of the mixed thiol-ene/homopolymerization crosslinking reaction with dithiothreitol (DTT, bottom) [Color figure can be viewed at wileyonlinelibrary.com]



modified according to following procedure. HA sodium salts were converted to tetrabutylammonium salts (HA-TBAs) by an ion exchange process in order to enhance solubility in DMSO. Subsequently, HA-TBAs were converted to hyaluronic acid vinyl esters (HA-VE) by a transesterification reaction with excessive divinyl adipate in anhydrous DMSO at 50 °C (Figure 1, top). All dissolution processes were performed by gentle agitation in order to avoid unwanted mechanically induced degradation.<sup>[39]</sup>

Reaction times were varied in order to obtain different degrees of substitution (DS) (Table 1). The DS was determined by selective vinyl ester hydrolysis recording <sup>1</sup>H NMR spectra in D<sub>2</sub>O in the presence of NaOD (Figure S1).<sup>[23]</sup> GPC elugrams of HA22VE95 and HA50VE05 before and after functionalization are depicted in Figure S2. This data indicate only a minor increase in molecular weight, which was expected to be a consequence of functionalization but also proved that the excess of DVA is sufficient as no interlinking of HA chains took place.

### 3.2 | Photorheological study

In order to investigate the influence of synthesis as well as formulation-originated parameters, photorheology was the method of choice. Photorheology is a versatile tool to investigate the photoreactivity and crosslink efficiency of hydrogel formulations.<sup>[40,45]</sup> Measurements were performed in oscillation mode by *in situ* photopolymerization of hydrogel formulations upon irradiation with filtered light (320–500 nm) through the bottom glass plate of the plate-to-plate measuring system. Important

system parameters were obtained from the storage modulus ( $G'$ ) curves.  $G'_{max}$  was used to calculate average mesh sizes  $L$  of the networks as a measure of the crosslink density of the hydrogels by Equation. (1).<sup>[46]</sup>

$$L = \left( \frac{R \cdot T}{G'_{max} \cdot N_A} \right)^{1/3} \quad (1)$$

Additionally, the slope ( $\Delta G' \Delta t^{-1}$ ), delay time ( $t_d$ ) and the time to reach 90% of  $G'_{max}$  ( $t_{G'_{max}^{90\%}}$ ) were calculated as described in literature to assess the quality of photopolymerization of the hydrogel systems.<sup>[40]</sup> The gel point  $t_g$ ,<sup>[47]</sup> was found to be equivalent to  $t_d$ , as no substantial increase of  $G'$  is observable before  $t_g$  is attained. LiTPO was used as photoinitiator. The synthesis and influence of LiTPO concentration are reported in Figure S3. Photoreactivities and crosslink densities increase dramatically with PI concentration. This is due to the higher concentration of radicals starting the polymerization. An optimum concentration of 0.05 wt.% LiTPO was used throughout the study. Complementary to the photorheological study the swellability of ready-cured hydrogels was investigated (Figure S7). Increasing swellability of the hydrogels was observed with decreasing DS as a result of increased mesh size and increased hydrophilicity.

### 3.3 | Macromer content, macromer chain length, and degree of substitution

Important structure parameter, which influence the reactivity and mechanical properties of the final hydrogels

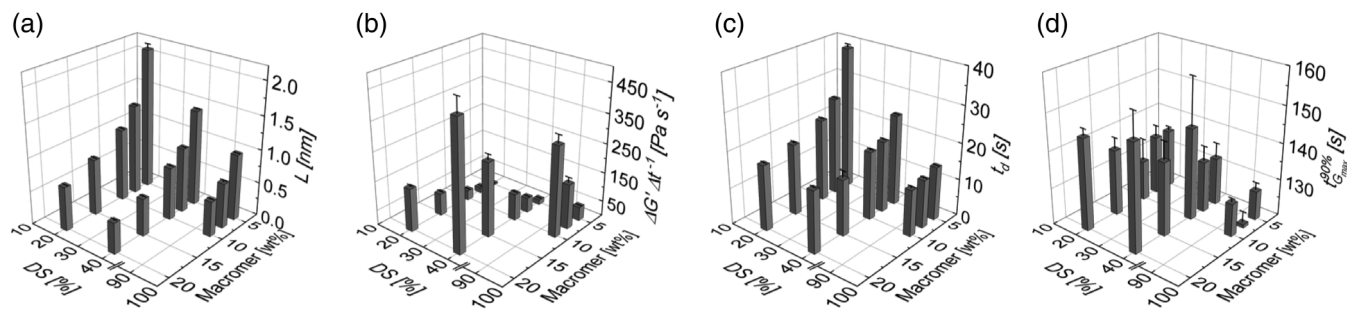


**FIGURE 2** Influence of the degree of substitution (DS) and the macromer content of HA hydrogel precursors with conserved  $\bar{M}n$  (22 kDa) on (a) the mesh size ( $L$ ) of the hydrogels, (b) slope of the storage modulus ( $\Delta G' \Delta t^{-1}$ ), (c) delay time ( $t_d$ ) and (d) the time to reach 90% of final storage modulus ( $t_{G_{max}^{90\%}}$ ). Error bars indicate the standard deviation of the measurements ( $N = 3$ )

are macromer content, macromer chain length ( $\bar{M}n$ ), and degree of substitution (DS). In order to investigate structure-properties relationships in this context a number of photorheology experiments were conducted, in which single parameter were varied while the others remained constant, resulting in two series of experiments, one set with conserved  $\bar{M}n$  (22 kDa) and the other set with conserved macromer content (5 wt.%). Considering DS and macromer content it was not possible to realize hydrogel formulations of HA22VE95 with contents 15 and 20 wt.% due to low processability owing to the high viscosity of solutions. For this reason, no rheological data is available for these formulations in Figure 2.

Generally, the data indicate that final crosslink densities (represented by the mesh size  $L$  in Figure 2a) and photoreactivities (represented by the slope of the storage modulus  $\Delta G' \Delta t^{-1}$  in Figure 2b) increased with DS as well as macromer content. The delay time  $t_d$  (Figure 2c) supports this data. This is elucidated by the increase of the number reactive groups when each of the parameter is increased and the increase of the number of chains by increasing the macromer content. While this trend was strictly followed by  $L$ ,  $\Delta G' \Delta t^{-1}$  and  $t_d$ , a disturbance was observed for  $t_{G_{max}^{90\%}}$  (Figure 2d). It is assumed that this parameter is highly sensitive to experimental variability also indicated by the relatively broad margin of error. However, the overall trend contributed to the proposed structure-properties relationship. Stressing the other combination of structure parameter (Figure S4)—DS and  $\bar{M}n$  all with 5 wt.% macromer content—again one data point is missing due to problems with viscosity, respectively. With the recent results in mind, it was not surprising that an increase in DS led to an increase in photoreactivity and final crosslink density also in case of formulations containing HA-VE with increased macromer size. However, the increase of macromer size itself also led to an increase of mentioned resulting parameters. This observation can be explained by the notional junction of HA backbones leading to additional

crosslinks and faster network formation, respectively. In other words, the probability that two reacting groups belong to one single chain, and therefore contribute to network formation, is higher for high molecular weight macromers.

### 3.4 | Thiol-ene chemistry

The photoreactivity of vinyl esters can be enhanced significantly by application of thiol-ene chemistry.<sup>[25]</sup> This was also shown previously for HA-VE using DTT as thiol reagent.<sup>[23]</sup> Moreover, by shifting the polymerization mechanism from a chain growth to a mixed chain/step growth reaction the uniformity of the network structure is increased leading to better mechanical properties.<sup>[24]</sup> In order to optimize the thiol-to-ene ratio the model system HA22VE95/DTT was analyzed by photorheology. Hydrogel precursor formulation with increasing molar ratio of thiol-to-ene (starting from 0 mol% to 120 mol% in 20 mol% steps) were prepared for these experiments. Formulations contained 5 wt.% macromer (also considering the mass of DTT) and 0.05 wt.% LiTPO as photoinitiator. Results from photorheology measurements are displayed in Figure 3.

The mesh size (Figure 3a) decreased (as a result of a higher crosslink density) and the photoreactivity increased (Figure 3b) with thiol content, in the first instance, however, a further increase of the amount of thiol led to a decrease in crosslink density and photoreactivity. The delay time (Figure 3c) and the time to reach 90% of the final storage modulus (Figure 3d) showed similar behavior. These findings are ascribed to the effect, that excessive amount of thiol led to a predominant ratio of mono-reacted groups and therefore retarded network formation leading to a decrease in the final crosslink density. The best results were found to be delivered by a ratio of 80 mol% thiols compared to ene.

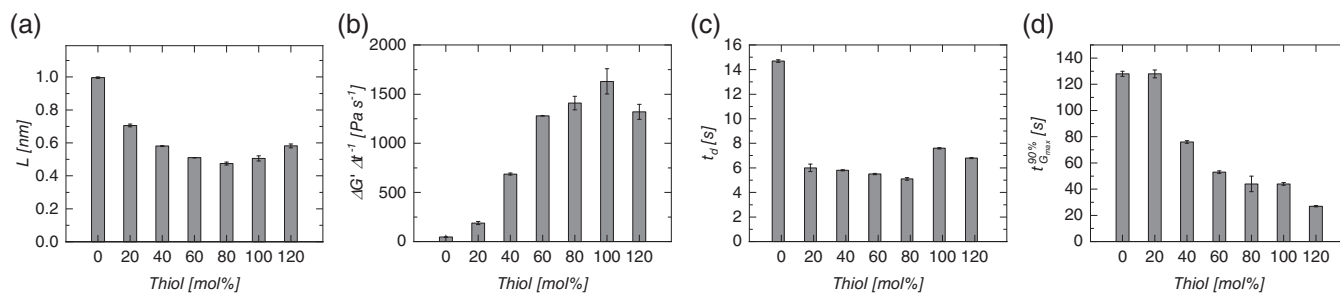
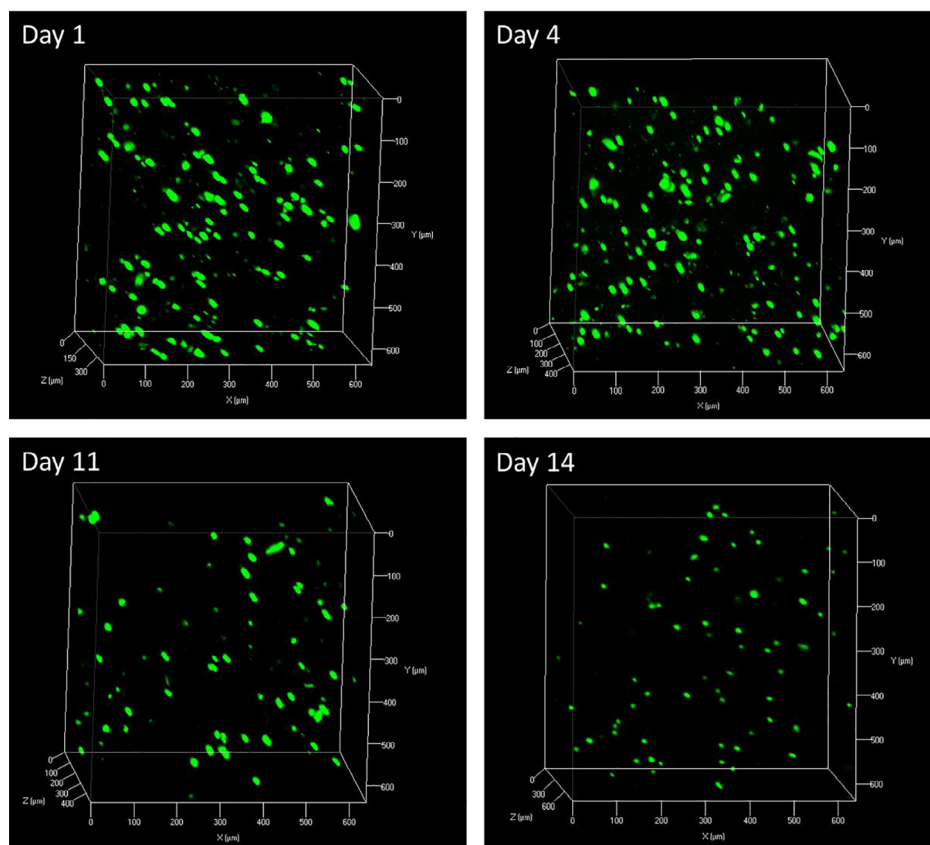


**FIGURE 3** Influence of the thiol molar ratio of hydrogel precursors (using HA22VE95/DTT systems with 5 wt.% gel content) on (a) the mesh size ( $L$ ) of the hydrogels, (b) slope of the storage modulus ( $\Delta G' \Delta t^{-1}$ ), (c) delay time ( $t_d$ ), and (d) the time to reach 90% of final storage modulus ( $t_{G_{max}^{90\%}}$ ). Error bars indicate the standard deviation of the measurements ( $N = 3$ )

**FIGURE 4** Confocal images of human adipose-derived mesenchymal stem cells labeled with green fluorescent protein (ASC-GFP) after UV encapsulation and 3D cultivation in HA-VE hydrogels for up to 14 days (HA50VE05/80 mol% thiol-to-ene DTT, 15 wt.% macromer content, 0.5 mM LiTPO<sup>[41]</sup>) [Color figure can be viewed at [wileyonlinelibrary.com](http://wileyonlinelibrary.com)]



With this knowledge, the influence of macromer content and DS on thiol-ene optimized formulations were investigated. In order to do this, formulations with 5.0, 7.5, and 10.0 wt.% HA22VE95 without and with 80 mol% DTT (thiol-to-ene) on the one hand and formulations with 10 wt.% of HA22VE20, HA22VE40, and HA22VE95 (including DTT, if applicable) again without and with 80 mol% DTT (thiol-to-ene) were prepared and tested by means of photorheology (Figures S5 and S6). In general, thiol-ene formulations exhibited the same trends for photoreactivity and mechanical properties compared to thiol-free formulations—the quality of photopolymerizations

is enhanced with macromer content as well as DS. However, the application of thiol-ene chemistry led to an increase of photoreactivity (assessed by  $\Delta G' \Delta t^{-1}$ ) by at least one order of magnitude and to a decrease of  $t_d$  (and the connected point of gelation) by a factor of about 4.

### 3.5 | UV cell encapsulation

In order to investigate material biocompatibility, ASC-GFPs were encapsulated in HA-VE hydrogels. Due to

enhanced solubility of HA-VE with moderate degree of substitution as well as m.w. and the increased chance to supply cells with a suitable surrounding microenvironment, HA50VE05 was chosen as material for UV cell encapsulation experiments. Due to the relatively low DS (5%) of HA50VE05, an increased amount of macromer content (15 wt.%) was selected in order to ensure sufficient crosslink density of the hydrogels. Photorheology curves of HA50VE05 representing conditions used for the UV-encapsulation of ASC-GFPs are depicted in Figure S12. First, a formulation based on HA50VE05 was prepared and mixed 1:1 (v/v) with cells in medium. Images of the prepared hydrogel pellets containing ASC-GFPs (Figure S13b) and a cell-free control (Figure S13a) is depicted in the Supporting Information. Gels were transferred to sterile  $\mu$ -dishes, immersed in cell medium and incubated at 37 °C up to 14 days. Cell-survival was monitored via LSM imaging. Cells were successfully encapsulated and monitored up to 14 days (Figure 4). Bright fluorescence of ASC-GFPs is observed over the course of 2 weeks.

The proliferation rate (cell number) was determined by counting the living cells using ImageJ within the recorded section ( $600 \times 600 \times 400 \mu\text{m}$ ). Cell numbers were counted on day 4, 11 and 14 and the data were normalized to day 1 (100%) (Figure S14, left). Cell numbers remained constant within the first 4 days (102%) and decreased up to day 11 (47%) and day 14 (38%) owing to swelling and disintegration of the hydrogel indicated by the low crosslink density originating from the low DS of HA50VE05. These arguments are confirmed by the swelling ratios as well as mass loss profiles depicted in Figure S9. Swelling ratio for HA50VE05 ( $928 \pm 31\%$ ) was observed to be twice as high as for HA22VE95 ( $479 \pm 16\%$ ). Additionally, mass loss profiles after 24 hr were calculated and a higher decrease of mass percentage was observed for HA50VE05 ( $25 \pm 4\%$ ) compared to  $7 \pm 4\%$  for HA22VE95. Round morphology of the cells was observed, which is most likely due to the missing cell-interactive properties of HA. Future experiments are planned to investigate interpenetrating hydrogel networks of HA-VE and gelatin incorporating protein motifs Arg-Gly-Asp (RGD) to enhance cell adhesion.<sup>[48–50]</sup>

### 3.6 | Cell encapsulation by two-photon polymerization

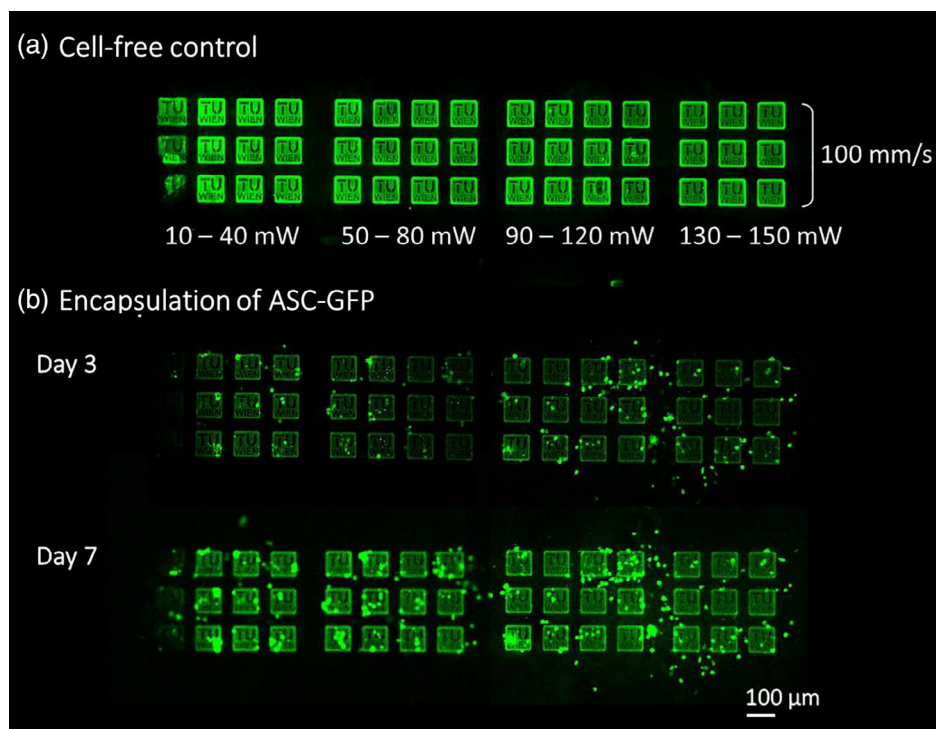
Encapsulation of ASC-GFP cells was performed in order to investigate cell viability in HA-VE hydrogels after the 2PP structuring process. For this, HA22VE95 with a high DS was chosen in order to ensure efficient photocrosslinking during 2PP. With remarkably high two-

photon absorption cross section (400 GM), P2CK is a very efficient two-photon initiator used for cell encapsulation.<sup>[42,51]</sup> Although, when used in high concentrations (10 mM) P2CK may also be applied in photodynamic therapy.<sup>[52]</sup> In order to maximize cell survival rate, minimal P2CK concentrations were chosen (0.5 mM). In order to encapsulate cells, a formulation based on HA22VE95 was prepared and mixed 1:1 (v/v) with cells in medium or PBS solution (cell-free control experiment). Contrary to UV encapsulation, 2PP-cell encapsulation experiments were performed using HA22VE95. Key reasons are the improved solubility of low-m.w. HA22VE95 (22 kDa) compared to HA50VE05 (50 kDa). Moreover, excellent performance during 2PP was observed for HA22VE95. Extremely high crosslink efficiencies during the high-speed 2PP structuring process were obtained as compared to HA50VE05 owing to the increased abundance of functional groups of HA22VE95. As proven by photorheology (Figure 2), improved crosslink densities are preferred especially when highly resolved 3D microstructures are monitored over a longer period of time (7 days). Due to the increased amount of hydrophobic (aliphatic) vinyl ester moieties introduced via modification, minimal amount of macromer content (5 wt.%) still applicable for 2PP was used enabling a more tolerable cell environment. Cubic hydrogel constructs ( $100 \times 100 \times 100 \mu\text{m}$  TU Wien Logos) were manufactured according to a CAD-file by scanning the focus of the laser beam of the 2PP device through the prepared formulation. By this, a suitable 3D microenvironment was fabricated including crosslinked hydrogel material as well as cavities in the shape of TU Wien letters. A suitable position within the precursor formulation was chosen in order to efficiently encapsulate cells within the material. Images of the printed constructs were captured via LSM up to 7 days (Figure 5).

A 2D-array was successfully fabricated in a reproducible quality by structuring logos with constant writing speed (y-axis) and varying laser power (x-axis). Structures in the cell-free control formulations were successfully printed with all laser power adjustments (10–150 mW). However, cell encapsulation hydrogel constructs printed with laser power < 20 mW seemed to be very fragile, which indicated a low crosslink density due to underexposure. Presumably, these structures were destroyed, detached and washed away during excessive rinsing procedures. Even though, round cell morphology was observed similar to UV cell encapsulation (Figure 4) numerous viable ASC-GFP cells were imaged for up to 7 days of incubation. In order to quantify the cells, structures were divided into 4 groups (10–40 mW; 50–80 mW; 90–120 mW; 130–150 mW). In particular, cells were counted, which were located inside of TU Wien Logos



**FIGURE 5** Laser scanning microscopy images of hyaluronic acid-based hydrogel constructs (HA22VE95/80 mol% thiol-to-ene DTT, 5 wt.% macromer content), printed with varied laser powers ( $\Delta = 10$  mW) and a constant writing speed of  $100 \text{ mm s}^{-1}$  (triplicates) according to a CAD-model (TU Wien Logo,  $100 \times 100 \times 100 \mu\text{m}$ ) in the presence of  $0.5 \text{ mM}$  P2CK (cell-free control, a). Fluorescent-labeled ASCs were imaged after 3 and 7 days of encapsulation (b) [Color figure can be viewed at [wileyonlinelibrary.com](http://wileyonlinelibrary.com)]



including cells located at the edges of 3D microstructures however, excluding cells on the glass surface outside of the structures. Cell numbers were counted on day 7 and the data were normalized to day 3 (100%). Higher cell proliferation rates were observed for structures, which were produced with lower laser power (10–40 mW) compared to structures, which were fabricated with relatively high laser power (120–150 mW) expected to be derived from the stiffer hydrogel structures. However, on average an overall cell number-increase of 26% across all applied laser powers was observed (Figure S14).

## 4 | CONCLUSIONS

In this study, the synthesis and characterization of hyaluronic acid-based hydrogels is shown. A straightforward synthesis method was developed obtaining macromers with multiple parameters open for variation. Hyaluronic acid vinyl esters were synthesized by means of acidic degradation, resulting in different macromer sizes and by subsequent transesterification reaction leading to macromers with a different degree of substitution. By consideration of the variation of aforementioned synthesis parameter and the variation of formulation parameter, including photoinitiator concentration, macromer content, and thiol-to-ene ratio, structure–property relationships of the complex thiol-ene based photopolymer system were elucidated by means of photorheology studies. Generally, photoreactivity as well as crosslink density increased with

the macromer size, the degree of substitution, the photoinitiator concentration, and the macromer content. Overall, a higher abundance of functional groups combined with an increased concentration of radicals lead to denser networks. However, an optimum thiol-to-ene ratio was found to be at 80 mol%. Swellabilities of ready-cured hydrogels followed the trend as expected from calculated mesh sizes of the networks on the basis of rheological data. The swellability of the hydrogels increased with decreasing DS as a result of increased mesh size and increased hydrophilicity. Solubility of macromers is highly dependent on initial molecular weight as well as degree of modification owing to the change of hydrophilicity of the macromer chains after modification with hydrophobic (aliphatic) vinyl ester moieties. These investigations enabled the formulation of tailor-made hydrogel precursors leading to successful encapsulation of cells in HA-VE based 3D hydrogel constructs monitoring their cell survival after the encapsulation process. Two different HA-VEs were chosen in order to perform UV and 2PP cell encapsulation experiments, respectively. HA50VE05 with a m.w. of 50 kDa was found to be an excellent candidate for UV cell encapsulation. By using higher macromer concentrations (15 wt.%) but lower DS (5%) relatively soft hydrogels were prepared, especially suited for cell culture ensuring pleasant cell-environment comparable to ECM. ASC-GFPs were successfully encapsulated in bulk HA-VE pellets and their viability was studied for up to 14 days. Numerous viable cells were observed over the whole course although high degree of swelling was observed for

HA50VE05. On the other hand, low m.w. HA22VE95 (22 kDa) was found to be an optimum material for 2PP cell encapsulation with good solution properties, when used in low macromer concentrations (5 wt.%) while maintaining consistent quality of crosslinking owing to the high DS (95%). Highly resolved hydrogel microstructures ( $100 \times 100 \times 100 \mu\text{m}$  TU Wien Logos) were fabricated with enhanced long-term stability. ASC-GFPs were successfully encapsulated via 2PP and their survival monitored for up to 7 days. Good cell proliferation rates were observed for all different structuring parameters, however, microstructures fabricated with higher laser power resulted in stiffer hydrogel constructs with reduced cell proliferation rates; Structures fabricated with lower laser power led to softer hydrogels prone to disintegration as a result of the low crosslink density yet showing increased cell proliferation rates. This study illustrates how HA-VE is expected to be one versatile contributor in the broad field of hydrogel materials. Further studies will increase the knowledge of the system and enhance its properties toward the potential application in the fields of tissue engineering and regenerative medicine.

## ACKNOWLEDGMENTS

The financial support by the Austrian Federal Ministry for Digital and Economic Affairs and the National Foundation for Research, Technology and Development is gratefully acknowledged. The authors would also like to thank the Austrian Research Promotion Agency (FFG, projects “3DFabBio”, number 1362110 and “Hydroceram”, number 849787). The authors thank Dr. Severin Muehleider and Prof. Wolfgang Holnthoner (Ludwig-Boltzmann-Institute for Experimental and Clinical Traumatology, Vienna, Austria) for their help with cell transfection.

## ORCID

Stefan Baudis  <https://orcid.org/0000-0002-5390-0761>

## REFERENCES

- [1] H. K. Kleinman, D. Philp, M. P. Hoffman, *Curr. Opin. Biotechnol.* **2003**, *14*, 526.
- [2] C. A. DeForest, K. S. Anseth, *Ann. Rev. Chem. Biomol. Eng.* **2012**, *3*, 421.
- [3] R. O. Hynes, *Science (New York, N.Y.)* **2009**, *326*, 1216.
- [4] J. J. Rice, M. M. Martino, L. De Laporte, F. Tortelli, P. S. Briquez, J. A. Hubbell, *Adv. Healthcare Mater.* **2013**, *2*, 57.
- [5] B.-S. Kim, D. J. Mooney, *Trends Biotechnol.* **1998**, *16*, 224.
- [6] M. P. Lutolf, J. A. Hubbell, *Nat. Biotech.* **2005**, *23*, 47.
- [7] C. Werner, T. Pompe, K. Salchert, In *Polymers for Regenerative Medicine*; C. Werner, Ed.; Springer: Berlin, Heidelberg, **2006** Chap. 89.
- [8] T. C. Laurent, J. R. Fraser, *FASEB J.* **1992**, *6*, 2397.
- [9] J. A. Burdick, G. D. Prestwich, *Adv. Mater.* **2011**, *23*, H41.
- [10] M. N. Collins, C. Birkinshaw, *Carbohydr. Polym.* **2013**, *92*, 1262.
- [11] M. S. Shazeeb, R. Corazzini, P. A. Konowicz, R. Fogle, D. S. Bangari, J. Johnson, X. Ying, P. K. Dhal, *Biomaterials* **2018**, *178*, 326.
- [12] S. N. A. Bukhari, N. L. Roswandi, M. Waqas, H. Habib, F. Hussain, S. Khan, M. Sohail, N. A. Ramli, H. E. Thu, Z. Hussain, *Int. J. Biol. Macromol.* **2018**, *120*, 1682.
- [13] K. J. Wolf, S. Kumar, *ACS Biomater. Sci. Eng.* **2019**, *5*, 3753.
- [14] C. B. Highley, G. D. Prestwich, J. A. Burdick, *Curr. Opin. Biotechnol.* **2016**, *40*, 35.
- [15] S. Gerecht, J. A. Burdick, L. S. Ferreira, S. A. Townsend, R. Langer, G. Vunjak-Novakovic, *Proc. Natl. Acad. Sci.* **2007**, *104*, 11298.
- [16] S. Khetan, M. Guvendiren, W. R. Legant, D. M. Cohen, C. S. Chen, J. A. Burdick, *Natl. Mater.* **2013**, *12*, 458.
- [17] A. F. Jeffery, M. A. Churchward, V. K. Mushahwar, K. G. Todd, A. L. Elias, *Biomacromolecules* **2014**, *15*, 2157.
- [18] P. A. Levett, F. P. W. Melchels, K. Schrobback, D. W. Huttmacher, J. Malda, T. J. Klein, *J. Biomed. Mater. Res. A* **2014**, *102*, 2544.
- [19] W. M. Gramlich, I. L. Kim, J. A. Burdick, *Biomaterials* **2013**, *34*, 9803.
- [20] C. Heller, M. Schwentenwein, G. Russmueller, F. Varga, J. Stampfl, R. Liska, *J. Polym. Sci. A* **2009**, *47*, 6941.
- [21] B. Husar, C. Heller, M. Schwentenwein, A. Mautner, F. Varga, T. Koch, J. Stampfl, R. Liska, *J. Polym. Sci. A* **2011**, *49*, 4927.
- [22] G. Russmueller, R. Liska, J. Stampfl, C. Heller, A. Mautner, K. Macfelda, B. Kapeller, R. Lieber, A. Haider, K. Mika, C. Schopper, C. Perisanidis, R. Seemann, D. Moser, *Materials* **2015**, *8*, 3685.
- [23] X.-H. Qin, P. Gruber, M. Markovic, B. Plochberger, E. Klotzsch, J. Stampfl, A. Ovsianikov, R. Liska, *Polym. Chem.* **2014**, *5*, 6523.
- [24] C. E. Hoyle, A. B. Lowe, C. N. Bowman, *Chem. Soc. Rev.* **2010**, *39*, 1355.
- [25] A. Mautner, X. Qin, H. Wutzel, S. C. Ligon, B. Kapeller, D. Moser, G. Russmueller, J. Stampfl, R. Liska, *J. Polym. Sci. A* **2013**, *51*, 203.
- [26] S. B. Anderson, C.-C. Lin, D. V. Kuntzler, K. S. Anseth, *Biomaterials* **2011**, *32*, 3564.
- [27] C.-C. Lin, A. Raza, H. Shih, *Biomaterials* **2011**, *32*, 9685.
- [28] R. J. Wade, E. J. Bassin, W. M. Gramlich, J. A. Burdick, *Adv. Mater.* **2015**, *27*, 1356.
- [29] A. Dobos, J. Van Hoorick, W. Steiger, P. Gruber, M. Markovic, O. G. Andriotis, A. Rohatschek, P. Dubruel, P. J. Thurner, S. Van Vlierberghe, S. Baudis, A. Ovsianikov, *Adv. Healthcare Mater.* **2019**, 1900752. <https://doi.org/10.1002/adhm.201900752>.
- [30] X.-H. Qin, A. Ovsianikov, J. Stampfl, R. Liska, *Bio-NanoMaterials* **2014**, *15*, 49.
- [31] M. Tromayer, A. Dobos, P. Gruber, A. Ajami, R. Dedic, A. Ovsianikov, R. Liska, *Polym. Chem.* **2018**, *9*, 3108.
- [32] J. Stampfl, R. Liska, A. Ovsianikov, *Multiphoton Lithography: Techniques, Materials, and Applications*; Wiley, Germany, **2016**.
- [33] S. Basu, L. P. Cunningham, G. D. Pins, K. A. Bush, R. Taboada, A. R. Howell, J. Wang, P. J. Campagnola, *Biomacromolecules* **2005**, *6*, 1465.

- [34] K. A. Mosiewicz, L. Kolb, A. J. van der Vlies, M. M. Martino, P. S. Lienemann, J. A. Hubbell, M. Ehrbar, M. P. Lutolf, *Nat. Mater.* **2013**, *12*, 1072.
- [35] Y.-L. Sun, W.-F. Dong, L.-G. Niu, T. Jiang, D.-X. Liu, L. Zhang, Y.-S. Wang, Q.-D. Chen, D.-P. Kim, H.-B. Sun, *Light Sci. Appl.* **2014**, *3*, e129.
- [36] Y.-L. Sun, Q. Li, S.-M. Sun, J.-C. Huang, B.-Y. Zheng, Q.-D. Chen, Z.-Z. Shao, H.-B. Sun, *Nat Commun* **6**, 8612 **2015**. <https://doi.org/10.1038/ncomms9612>.
- [37] L. Knezevic, M. Schauppper, S. Mühleder, K. Schimek, T. Hasenberg, U. Marx, E. Priglinger, H. Redl, W. Holnthoner, *Front. Bioeng. Biotechnol.* **2017**, *5*, 25.
- [38] Sigma-Aldrich. Product Information of 3-(Trimethoxysilyl)propyl methacrylate [https://www.sigmaaldrich.com/content/dam/sigma-aldrich/docs/Sigma/Product\\_Information\\_Sheet/1/m6514pis.pdf](https://www.sigmaaldrich.com/content/dam/sigma-aldrich/docs/Sigma/Product_Information_Sheet/1/m6514pis.pdf) (accessed January 27, 2020).
- [39] M. N. Collins, C. Birkinshaw, *J. Appl. Polym. Sci.* **2013**, *130*, 145.
- [40] C. Gorsche, R. Harikrishna, S. Baudis, P. Knaack, B. Husar, J. Laeuger, H. Hoffmann, R. Liska, *Analytic. Chem.* **2017**, *89*, 4958.
- [41] S. Benedikt, J. Wang, M. Markovic, N. Moszner, K. Dietliker, A. Ovsianikov, H. Grützmacher, R. Liska, *J. Polym. Sci. A* **2016**, *54*, 473.
- [42] Z. Li, J. Torgersen, A. Ajami, S. Muhleder, X. Qin, W. Husinsky, W. Holnthoner, A. Ovsianikov, J. Stampfl, R. Liska, *RSC Adv.* **2013**, *3*, 15939.
- [43] H. M. Dyanov, S. G. Dzitoeva, *Biotechniques* **1995**, *18*, 822.
- [44] S. Baudis, D. Bomze, M. Markovic, P. Gruber, A. Ovsianikov, R. Liska, *J. Polym. Sci. A* **2016**, *54*, 2060. <https://doi.org/10.1002/pola.28073>.
- [45] B. D. Fairbanks, M. P. Schwartz, C. N. Bowman, K. S. Anseth, *Biomaterials* **2009**, *30*, 6702.
- [46] J. Wang, V. M. Ugaz, *Electrophoresis* **2006**, *27*, 3349.
- [47] H. H. Winter, *Polym. Eng. Sci.* **1987**, *27*, 1698.
- [48] A. Mora-Boza, M. Puertas-Bartolomé, B. Vázquez-Lasa, J. San Román, A. Pérez-Caballer, M. Olmeda-Lozano, *Eur. Polym. J.* **2017**, *95*, 11.
- [49] R. Tsaryk, A. Gloria, T. Russo, L. Anspach, R. De Santis, S. Ghanaati, R. E. Unger, L. Ambrosio, C. J. Kirkpatrick, *Acta Biomater.* **2015**, *20*, 10.
- [50] Z. Fan, Y. Zhang, S. Fang, C. Xu, X. Li, *RSC Adv.* **2015**, *5*, 1929.
- [51] J. Van Hoorick, P. Gruber, M. Markovic, M. Tromayer, J. Van Erps, H. Thienpont, R. Liska, A. Ovsianikov, P. Dubruel, S. Van Vlierberghe, *Biomacromolecules* **2017**, *18*, 3260.
- [52] A. Dobos, W. Steiger, D. Theiner, P. Gruber, M. Lunzer, J. Van Hoorick, S. Van Vlierberghe, A. Ovsianikov, *Analyst* **2019**, *144*, 3056.

## SUPPORTING INFORMATION

Additional supporting information may be found online in the Supporting Information section at the end of this article.

**How to cite this article:** Zerobin E, Markovic M, Tomášiková Z, et al. Hyaluronic acid vinyl esters: A toolbox toward controlling mechanical properties of hydrogels for 3D microfabrication. *J Polym Sci.* 2020;1–11. <https://doi.org/10.1002/pol.20200073>